Field ionization of neutral lithium vapor using a 28.5 GeV electron beam*

C.L. O'Connell [†], C. D. Barnes, F.-J. Decker, M.J. Hogan, R. Iverson,
P. Krejcik, R. Siemann, D.R. Walz, SLAC, Menlo Park, CA 94025, USA
S. Deng, T. Katsouleas, P. Muggli, E. Oz, USC, Los Angeles, CA 90089, USA
C.E. Clayton, C. Huang, D. K. Johnson, C. Joshi, W. Lu, K. A. Marsh, W. Mori, M. Zhou
UCLA, Los Angeles, CA 90095, USA

Abstract

The E164/E164X plasma wakefield experiment studies beam-plasma interactions at the Stanford Linear Acceleration Center (SLAC). Due to SLAC's recent ability to variably compress bunches longitudinally from 650 μm down to 20 μm, the incoming beam is sufficiently dense to field ionize the neutral lithium (Li) vapor. The field ionization effects are characterized by the beams energy loss through the Li vapor column. Experiment results are presented.

INTRODUCTION

Plasma-based accelerators utilizing relativistic propagating plasma waves, or wakes, offer the potential of higher acceleration gradients and stronger focusing fields as compared to conventional RF acceleration methods and magnetic focusing. The E164/E164X experiments at SLAC study the longitudinal and transverse dynamics of electron-bunch drivers in a dense plasma.

In the summer of 2002, a magnetic chicane was installed along the linac to longitudinally compress the electron bunch from the nominal value of 650 μm down to around 20 μm. As the bunch length gets shorter the acceleration gradient of the plasma wake increases. As discussed in a paper published by Bruhwiler *et al.*, once the beam is sufficiently short, self-fields of the beam are strong enough to ionize the Li vapor [1]. After the beam ionizes the vapor, it expels the plasma electrons due to its space-charge effects and generates its own plasma wake.

FIELD IONIZATION

An atom in an external electric field creates a potential barrier for the outermost electron. As the external electric field increases the width of the potential barrier decreases, increasing the probability that the outermost electron will tunnel through the barrier.

The rate of field ionization is related to the peak radial electric field, F_{peak}, of the incoming electron beam. F_{peak} for a Gaussian bunch along r and z can be conveniently summarized into the following engineering formula

$$F_{peak} \approx 10.4 \, \frac{GV}{m} \left[\frac{N}{1 \times 10^{10}} \right] \left[\frac{10 \, \mu m}{\sigma_r} \right] \left[\frac{50 \, \mu m}{\sigma_z} \right] \quad (1)$$

where N is the number of electrons per bunch, σ_r is the transverse spot size and σ_z is the bunch length.

The Ammosov, Delone and Krainov (ADK) approximation relates the beam's electric field with the ionization rate. The technique is a fully-generalized, quasi-classical approximation of the tunneling ionization rate for complex atoms in an alternating (AC) electric field [2]. The initial arbitrary state for the complex atom is described by an effective quantum number, $n^* = Z/\sqrt{2\varepsilon_0}$, where Z is the charge of the atomic residue (e.g. one for first ionization and two for secondary ionization), ε_0 is the ionization energy of the atom, as well as the angular and magnetic quantum numbers ℓ and m, respectively. The instantaneous ADK tunneling rate, in atomic units, is

$$
\begin{aligned}
W_{ADK} = \quad & C_{n^*\ell}^2 \frac{(2\ell+1)(\ell+|m|)!}{2^{|m|}|m|!(\ell-|m|)!} |\varepsilon_0| \\
& \times \left(\frac{2(2|\varepsilon_0|)^{3/2}}{F} \right)^{2n^*-|m|-1} \\
& \times \exp\left(-\frac{2(2|\varepsilon_0|)^{3/2}}{3F} \right) \quad , \quad (2)
\end{aligned}
$$

where

$$C_{n^*\ell} = \left(\frac{2e}{n^*} \right)^{n^*} (2\pi n^*)^{-1/2} \quad . \quad (3)$$

The constant e in the coefficient $C_{n^*\ell}$ is Euler's number 2.718. The validity of the ADK formula is expected to be best in the quasi-classical approximation, $n^* \gg 1$. However, the approximation is accurate to a few percent up to values of $n^* \approx 1$.

Once ionization occurs, the plasma electrons are expelled due to the space-charge effects of the beam. Without plasma production, the beam would pass through the plasma source section without any interaction, as if it were a drift section. Consequently, the field ionization effects are characterized by the beam's energy loss through the lithium vapor column due to the plasma wake production.

EXPERIMENTAL METHOD

SLAC's E164/E164X experiments use a 28.5 GeV electron beam at the Final Focus Test Beam (FFTB) Facility. Figure 1 illustrates the primary features of the experimental setup. The beam first traverses a chicane located within a high-dispersion region. The beam emits synchrotron radiation, which is captured and imaged. This allows for a

non-destructive determination of the beam's incoming energy spread. Ahead of the plasma source is a 1 μm titanium foil which generates transition radiation. At wavelengths longer than the bunch length the transition radiation becomes coherent (CTR) and the integrated CTR energy increases as the bunch length becomes shorter.
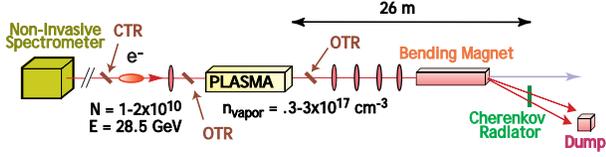

Figure 1: Schematic of the experimental layout. The diagram is not to scale.

The beam is focused transversely before entering the plasma source. The latter is a 6-10 cm long heat-pipe oven filled with Li vapor with densities of $0.3 - 3 \times 10^{17}$ cm^{-3}. A magnetic energy spectrometer images the beam at the plasma exit onto a thin piece of aerogel located some 25 m downstream. The resulting Cherenkov light is collected and imaged onto a charge-coupled device (CCD) camera, where the vertical axis of the image is dominated by the beam's energy spread. See Table 1 for the typical beam and plasma parameters.

Table 1: Typical beam and plasma parameters

Number of e$^-$ per bunch	N	$0.6 - 1.6 \times 10^{10}$
Bunch Energy	E, γ	28.5 GeV, 5.6×10^4
Bunch Length [μm]	σ_z	$20 - 110$
Vapor Density [cm^{-3}]	n_v	$0.3 - 3.0 \times 10^{17}$
Plasma Oven Length [cm]	L	$6 - 10$

EXPERIMENTAL RESULTS

As seen in Equation 1, F_{peak} is proportional to N and inversely proportional to σ_z and σ_r. The radial electric field is controlled to be above or below the threshold for field ionization by independently varying each one of these three parameters.

Changing Charge

Holding σ_r and σ_z constant and varying N, the electric field is increased until the field ionization threshold is crossed. For the data presented, $\sigma_r \approx 20$ μm. Variations in the transverse size of the incoming beam is related to emittance changes with charge and inherent jitter of the two-mile long linear accelerator's output. Using the LiTrack simulation code [3] to determine σ_z, the charge distribution had a mathematical standard deviation of 56 μm, but the center peak was approximately 26 μm. The charge of

the incoming bunch was varied from $0.6 - 1.43 \times 10^{10}$ electrons per bunch. Figure 2 illustrates the two states for the incoming beam.
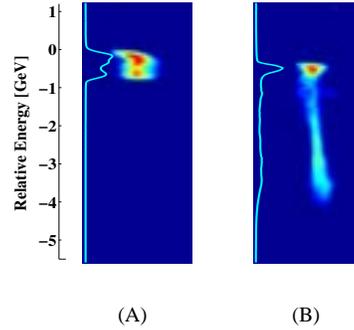

(A) (B)

Figure 2: The images are plotted with a logarithmic color map in order to bring out the tails. (A) $N = 0.61 \times 10^{10}$ and no ionization occurs. (B) $N = 1.43 \times 10^{10}$ fully ionizes the Li vapor.

The two images in Figure 2 show the bunch's energy spectrum at the Cherenkov radiator, where the more energetic particles are at the top of the image. The field ionization effects are characterized by the significant amount of energy loss observed at the Cherenkov radiator when the incoming beam is sufficiently dense. In both images, the vertical profile is superimposed along the left edge of the image.
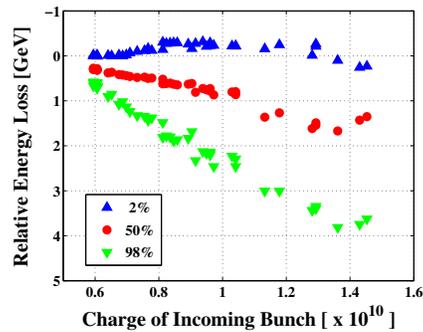

Figure 3: Changing Charge − Plotting the 2%, 50% and 98% charge levels along the energy (vertical) component of the Cherenkov diagnostic.

The data plotted in Fig. 3 was acquired at a rate of 1 Hz over a period of two hundred seconds. In order to limit variations in the incoming bunch length, tight cuts were made on a normalized CTR signal (CTR Energy/N^2), which reduced the data set from 200 events down to 48. Figure 3 accumulates the vertical profiles for the remaining 48 events and sorts them by increasing charge. Three distributions levels are plotted: 2%, 50% and 98%. Each level is defined as the location which contains 2%, 50%, and 98% of the charge and is obtained by taking a running sum of the charge from the top to the bottom of the Cherenkov

image. The zero energy loss is defined as the 2% level for the non-ionizing case (up-arrows). The average energy loss is defined as the energy where 50% of the charge registered on the detector is located (circles) and the peak energy loss is defined as the 98% mark (down-arrows). For the highest charge, the average energy loss of the bunch was 1.5 GeV and peak energy loss between the extreme cases was ≈ 3.5 GeV . The ionization threshold is reached at $N \approx 0.65 \times 10^{10}$ for the constant values of σ_r and σ_z.

Changing Bunch Length

As σ_z decreases and the other parameters are held constant, the electric field increases and the threshold conditions are sufficient to ionize the Li vapor. For the data set presented, N is held constant at $\approx 8.75 \times 10^9$ and σ_r is held around 15 μm. Again, any variations are due to the inherent emittance jitter of the machine. To determine the relative σ_z of the incoming electron bunches, the data events are sorted according to increasing CTR energy, where an increasing signal indicates a decreasing σ_z.
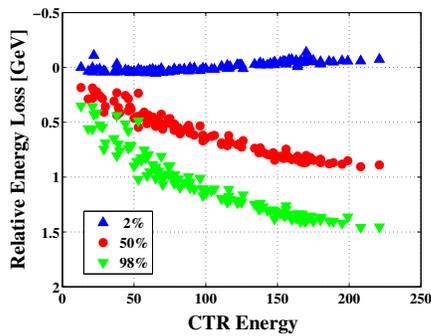

Figure 4: Changing Bunch Length − Plotting the 2%, 50% and 98% charge levels along the energy (vertical) component of the Cherenkov diagnostic.

The data set plotted in Fig. 4 was acquired at a rate of 1 Hz for 200 seconds. Cuts on charge reduced the data set to 122 events. According to LiTrack results, σ_z was varied from ≈ 105 μm down to 25 μm. The field ionization threshold occurs for $\sigma_z \approx 66$ μm, which corresponds to a CTR energy GADC count of 29. Figure 4 accumulates the vertical profiles for the remaining 122 events and sorts them according to CTR energy, where zero is the registered signal level on the diagnostic for no beam. For the shortest lengths produced, the bunches lost an average of 800 MeV. A peak energy loss of approximately 1.2 GeV between the non-ionized and full-ionized cases was observed.

Changing Spot Size

As the σ_r of the incoming bunch gets smaller, the radial electric field increases until the incoming bunch ionizes the Li vapor. To observe this threshold, the waist location for the incoming beam is varied along the z-axis by altering two quadrupoles upstream of the plasma entrance. For the

data set described, the waist was moved from 45 cm upstream of the plasma entrance to 55 cm downstream of the plasma entrance, in 5 cm increments with 10 shots taken at each step. While varying the waist location, tight cuts were made on the CTR energy GADC count and charge to ensure σ_z and N were held constant. This reduced the data set from 200 to 103. For the data presented, $\sigma_z \approx 35$ μm for the center peak Gaussian, accordingly to LiTrack, with a mathematical standard deviation of 64 μm, and N was $\approx 8.8 \times 10^9$ electrons per bunch.

The change in σ_r from the smallest value with the waist at the plasma entrance to largest with the waist pulled 55 cm downstream is from about 10 μm up to approximately 50 μm. Figure 5 plots the three distributions for each event's vertical profile onto a single graph. The vertical axis of the graph is the waist location of the beam with respect to the plasma entrance in units of centimeters, where the entrance is located at the zero mark. At the smallest σ_r, the bunch lost an average energy of 600 MeV and a peak energy loss of 800 MeV between the two extreme cases.
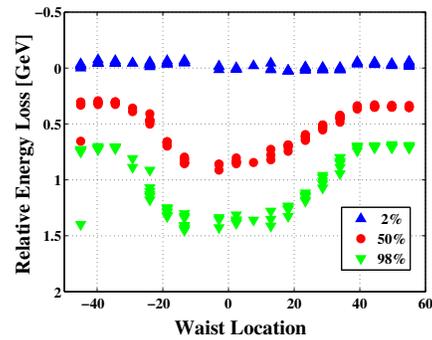

Figure 5: Changing Spot Size − Plotting the 2%, 50% and 98% charge levels along the energy (vertical) component of the Cherenkov diagnostic.

CONCLUSIONS

A beam-ionized plasma is a self-contained system, eliminating issues of alignment or timing. It allows for the scalability of the plasma length, which is an essential step for plasma wake field accelerators.

REFERENCES

[1] D.L. Bruhwiler *et al.*, "Particle-in-cell simulations of tunneling ionization effects in plasma-based accelerators," Physics of Plasmas 10(2003) 2022-2030.

[2] M.V. Ammosov, N. B. Delone and V. P. Krainov, "Tunnel ionization of complex atoms and of atomic ions in an alternating electromagnetic field," Sov. Phys. JETP 64 (1986) 1191-1194.

[3] P. Emma and K. Bane, "LiTrack: A Fast Longitudinal Phase Space Tracking Code with Graphical User Interface," PAC'05, Knoxville, TN, May 2005.